scientific reports

Check for updates

OPEN

Unveiling the role of TCF19 in intervertebral disc degeneration with single-cell and bulk RNA sequencing

Xianwei He[1], Liwei Wu[2]✉ & Hao Zhou[3]✉

Intervertebral disc degeneration (IDD) is a prevalent cause of low back pain, significantly impacting health worldwide. While IDD is associated with aging, its precise molecular mechanisms remain inadequately understood, limiting the development of targeted therapies. Nucleus pulposus cells (NPCs) are crucial to maintaining disc integrity and are central to understanding IDD progression. This study used single-cell and bulk RNA sequencing to dissect the cellular landscape and gene expression profiles in IDD. By analyzing these data, we identified distinct NPC subtypes and their roles in the degenerative disc microenvironment. Pseudotime and cellular communication network analyses further elucidated the temporal progression and signaling interactions of NPCs during disc degeneration. Four critical genes—TCF19, GDF15, RNMT, and C12orf45—were identified as significantly upregulated in IDD. TCF19 emerged as a key gene in the transitional states of NPCs, suggesting its pivotal role in IDD progression. In vivo experiments using a rat model indicated that Tcf19 knockdown significantly mitigated disc degeneration, reducing both abnormal collagen deposition and inflammation markers. This study unveils the complex molecular dynamics within IDD, providing new insights into distinct NPC subtypes and key genetic players. TCF19, in particular, holds promise as a therapeutic target for IDD. Our findings lay the groundwork for developing targeted treatment strategies, potentially improving the management and outcomes for individuals suffering from disc degeneration.

Keywords Intervertebral disc degeneration (IDD), Nucleus pulposus cells (NPCs), Single-Cell transcriptomics, Bulk sequencing, Cell communication, TCF19

Intervertebral disc degeneration (IDD) is an increasingly prevalent condition associated with aging, contributing significantly to the global burden of low back pain and disability[1–4]. The underlying molecular mechanisms, however, remain incompletely understood, challenging the development of targeted therapies. The complexity of IDD arises from its multifactorial nature, involving cellular dysfunction, aberrant extracellular matrix remodeling, and altered biomechanical forces[5–12].

Recent advances in single-cell RNA sequencing (sc-RNA-seq) have provided unprecedented insights into the cellular heterogeneity and complex intercellular communication networks within the degenerating intervertebral disc[8,13–16]. Specifically, nucleus pulposus cells (NPCs), which maintain the structural and functional integrity of the disc, have been identified to play critical roles in IDD progression. Yet, a comprehensive understanding of the changes occurring at the single-cell level in NPCs and their contribution to the degenerative processes remains to be elucidated[1,5,7,9].

In this study, we leveraged single-cell and bulk RNA sequencing to dissect the cellular landscape and gene expression patterns in IDD. Our investigation entailed the identification of distinct NPC subtypes and their differential gene expression profiles, providing a nuanced view of the disc microenvironment during degeneration. Moreover, we integrated bulk-seq data to pinpoint key differentially expressed genes, narrowing down potential therapeutic targets.

[1]Department of Orthopedic, Jinshan Hospital, Fudan University, Shanghai, China. [2]Heart Center and Shanghai Institute of Pediatric Congenital Heart Disease, Shanghai Children's Medical Center, National Children's Medical Center, Shanghai Jiao Tong University School of Medicine, Dongfang Road 1678#, Pudong district, Shanghai, China. [3]Department of Orthopedic, Shanghai Xuhui Central Hospital, Zhongshan-Xuhui Hospital, Fudan University, North Longchuan Road 366#, Xuhui district, Shanghai, China. ✉email: docwuliwei@foxmail.com; drzhouhao@163.com

We further employed pseudotime and cellular communication network analyses to decipher the temporal progression of cellular states and the intricate web of signaling interactions, respectively, enhancing our understanding of the pathophysiological narrative of IDD. Validation of our findings through quantitative PCR, ELISA, and Western Blot techniques solidified the role of specific genes and pathways, particularly highlighting the prognostic and therapeutic potential of identified biomarkers.

Through this integrative multi-omic approach, our study aims to illuminate the complex molecular orchestration of IDD, providing a foundation for novel diagnostic and therapeutic strategies that could alleviate the suffering associated with this debilitating condition.

Materials and methods

Acquisition of single-cell sequencing data and bulk RNA sequencing data

Single-cell sequencing data (GSE199866) and bulk RNA sequencing data (GSE186542) were acquired from the GEO database (https://www.ncbi.nlm.nih.gov/geo/). The bulk RNA sequencing data dataset comprised a total of 6 samples from individuals diagnosed with IDD, including 3 samples from early-stage degeneration (Pfirrmann's MRI grade: I-III) and 3 samples from advanced-stage degeneration (Pfirrmann's MRI grade: IV-V). These samples were utilized for the comprehensive analysis. The raw data were formatted as standard 10X Genomics files, which were then processed to generate Seurat objects for downstream analysis.

Identification of nucleus pulposus cell (NPC) functional subtypes and immune landscape in IDD

Analysis was conducted using the Seurat R package. The expression matrix was filtered to remove cells with overexpressed genes or excessive sequencing depth using the following criteria: nCount_RNA > 1000 & nFeature_RNA < 5000 & percent.MT < 30 & nFeature_RNA > 600. PCA reduction and UMAP reduction techniques were then employed to cluster all cells, with the clustered cells annotated according to cluster marker genes. NPCs were specifically extracted for further PCA and UMAP reduction analysis. Pseudotime analysis was carried out using the Monocle R package, aimed at exploring the trajectory of gene expression changes within NPCs, which can simulate the changes in gene expression over time at the single-cell level. The BEAM function in Monocle was utilized to investigate specific gene expression changes along the NPC trajectory.

Construction of intercellular communication networks among NPCs

The analysis was performed using the CellChat R package. Preprocessed single-cell RNA-seq data were input into CellChat, which identified potential ligand-receptor pairs by consulting CellChatDB, a comprehensive database of known and predicted cell-cell communication signals, including cytokines, growth factors, and their receptors. All NPCs were selected as the focus of intercellular communication analysis to explore the communication networks within the disc environment.

Acquisition of blood and tissue samples for IDD study

We collected whole blood samples from 15 patients diagnosed with IDD at the Orthopedics Department of Jinshan Hospital in Shanghai, while also collecting whole blood samples from 15 healthy individuals at the Health Examination Center of the same hospital to serve as a control group. All 15 IDD patients were male, aged between 68 and 79 years old, and were confirmed to have L2-L4 lumbar spine degeneration (Pfirrmann's MRI grade: III-IV). The control group of 15 healthy individuals included 8 males and 7 females, aged between 45 and 55 years. All the 15 IDD patients underwent surgical treatment with the removal of degenerative intervertebral discs, and these disc tissue samples were collected for subsequent experiments. The disc tissues for the control group were obtained through body donation, and we collected non-degenerative lumbar intervertebral discs as controls. Whole blood samples were collected on the first day of hospital admission, and plasma was extracted for subsequent experiments. All procedures involving human participants were approved by the Jinshan hospital ethics committee, with informed consent obtained from all subjects involved in the study. The clinical information of 15 IDD patients was presented in Table 1.

Animal model

Male Sprague-Dawley rats (8 weeks old), weighing 200–250 g, were used to establish an IDD model. All procedures were approved by the Institutional Animal Care and Use Committee and adhered to approved animal welfare guidelines. The rats were anesthetized with an intraperitoneal injection of ketamine (80 mg/kg) and xylazine (10 mg/kg). In a prone position, the surgical site around the lumbar spine was shaved and disinfected using povidone-iodine followed by 70% ethanol. The intervertebral disc between the sixth and seventh caudal vertebral body (Co6/7) of rats were located, and puncture was carried out with a 21G needle in the following discs following local disinfection. The puncture needle penetrated both sides of the annulus fibrosus and was hold for 30 s. Co6/7 was used as the own control. Then, 10 μl of AAV-Tcf19-shRNA (1.2×10^{12}vg/ml) was injected into Co7/8 using a 31G insulin needle. Disc degeneration was evaluated at predetermined time points (3 weeks after AAV injection) using histological examination following euthanasia. The rats were euthanized by being injected with an overdose of ketamine.

Histological evaluation

Disc samples from rats were fixed with 4% buffered formaldehyde, decalcified with 10% ethylenediaminetetraacetic acid (EDTA, Solarbio, China) for 1 month, and embedded in paraffin. For histological analysis, sections of 5 μm thickness were stained with hematoxylin-eosin (H&E), Alcian, safranin-O (SO) and fast green to evaluate morphology and proteoglycan distribution.

Characteristics	$n = 15$
Age	74.6 ± 2.84
Gender	
Male	15
Female	0
Spine level	
L1	0
L2	4
L3	6
L4	5
L5	0
Pfirrmann's MRI grade	
I	0
II	0
III	6
IV	9
V	0

Table 1. The clinical information of 15 IDD patients.

Gene ID	Gene Name	Forward Primer	Reverse Primer	Cycle	Annealing temperature
121,053	C12orf45	ACC-AGA-ACT-GTA-CAC-AGC-CG	CCT-ACT-GTG-CAC-CAC-ACA-CT	35	58℃
8731	RNMT	ACC-AAA-ATC-TCA-GCT-TCA-CAA-AGT	CCA-GTC-CCA-GAA-GCT-GTT-GT	35	58℃
9518	GDF15	GCA-AGA-ACT-CAG-GAC-GGT-GA	TGG-AGT-CTT-CGG-AGT-GCA-AC	35	58℃
6941	TCF19	CGC-GGT-GGA-TTC-ATT-GCC	ATA-GAG-CAC-TCC-TGC-TTG-CC	35	58℃
2597	GAPDH	GAA-GGT-GAA-GGT-CGG-AGT-CAA-C	CAG-AGT-TAA-AAG-CAG-CCC-TGG-T	35	58℃

Table 2. The primers of candidate genes.

Immunofluorescence

The sections were incubated with a sodium citrate buffer overnight at 65 °C for antigen retrieval. After permeabilization and blocking, the slides were incubated with primary antibodies overnight at 4 °C and then labeled with secondary antibodies for 2 h at room temperature. The following primary antibodies were used: anti-Collagen X from Invitrogen (catalog #PA5-115039) and anti-MMP13 from Invitrogen (catalog #PA5-27242). The following secondary antibodies were used: Goat anti-Rabbit 488 IgG from Invitrogen (catalog #A-11008).

Real-time quantitative polymerase chain reaction (RT-qPCR)

The total RNA was extracted from the tissues (human disc samples) using an RNA extraction kit (no. R701-01, Vazyme) following the manufacturer's instructions. Reverse transcription was performed using a Primescript RT reagent kit (no. RR047Q, Takara), while the Life Technology ABI 7500 System based on SYBR-Green PCR kit (no. A25742, Thermo Fisher Scientific) was used for qPCR. The δδCT method was used for calculating the gene expression relative to a housekeeping gene. The primer sequences used in the RT-qPCR are presented in the Table 2.

Western blot analysis

For Western blotting, the following primary antibodies were used: anti-TCF19 (37 kDa) obtained from Abcam (catalog #ab96828) and anti-Tubulin (50 kDa) also from Abcam (catalog #ab7291) as a loading control. The proteins were transferred to polyvinylidene fluoride (PVDF) membranes, which were then blocked and incubated with the primary antibodies. Appropriate horseradish peroxidase (HRP) conjugated secondary antibodies were applied, and the protein bands were visualized using enhanced chemiluminescence.

ELISA

For quantitative determination of protein concentration, ELISA was performed using the ThermoFisher FN1 ELISA Kit (catalog #BMS2028) according to the manufacturer's protocol. Samples and standards were prepared, and the assay was performed to allow for the detection and quantification of the target protein within the sample.

Statistical analysis

All analyses were performed using R software (version 4.2.2). Functional annotation of gene lists was conducted using the Metascape database (https://metascape.org), with results visualized using the ggplot2 R package. Data analysis was further supported by Prism 9 software, with statistical significance determined by Student's t-test and one-way ANOVA. A p-value of < 0.05 was considered statistically significant.

Results

Single-Cell RNA atlas of IDD

We conducted analysis based on GSE199866 (single-cell RNA sequencing data on samples from IDD patients and healthy individuals), successfully capturing 9845 high-quality cells for comprehensive analysis. Through the application of UMAP for dimensionality reduction, these cells were categorized into 4 major types of NPCs (Fig. 1A) and 7 distinct clusters (Fig. 1B). The comparative UMAP plots of IDD and healthy disc tissues, presented in Fig. 1C, revealed significant heterogeneity, underscoring diverse cellular functionalities and the formation of a disc microenvironment that might influence degenerative processes. We analyzed the proportion of each type of NPCs in the IDD group and the normal group and found that the proportion of regulatory NPCs and effector NPCs was significantly higher in the IDD group, while hypertrophy chondrocyte-like NPCs (HT-CLNPs) had a significantly higher proportion in the normal group. The proportion of fibro NPCs showed little difference between the two groups (Fig. 1D). The marker genes showcased in Fig. 1E. *SPP1* was a marker gene for effectors (Fig. 1F). *FRZB* was a marker gene for HT-CLNPs (Fig. 1G). *COL1A2* was a marker gene for fibro NPCs (Fig. 1H). *IL11* was a marker gene for regulatory NPCs (Fig. 1I). To further explore the functions of each type of NPC, we conducted a gene set variation analysis (GSVA). Fibro NPCs primarily undertake collagen-related functions, regulatory NPCs are mainly responsible for immune regulation functions, HT-CLNPs are primarily enriched in extracellular matrix synthesis functions, and effector NPCs are mainly enriched in metabolism-related functions (Fig. 1J).

Further subtyping of fibro NPCs in IDD

In our focused analysis of fibro NPCs within the context of NP, further dimensional reduction and clustering techniques were applied, revealing the subdivision of fibro NPCs into four distinct subclusters, as depicted in Fig. 2A. Subsequently, a heatmap analysis of gene expression similarity among these subclusters allowed for their categorization into three functional subgroups, showcased in Fig. 2B. Comparative UMAP plots across different disease states and healthy control groups displayed in Fig. 2C, illustrated the heterogeneity within fibro NPCs across these conditions. The UMAP representation of these functional clusters (FC) is vividly illustrated in Fig. 2D, highlighting the distinct gene expression profiles characteristic of each subgroup. To further explore the proportions of the three types of FCs in the IDD group and the normal group, we found that FC3 and FC2 almost entirely originated from the IDD group, while FC1 mainly came from the normal group (Fig. 2E). We used GSVA to evaluate the functions and pathways enriched in the three types of FC. FC1 was primarily enriched in "Immune complex clearance" and "ficolins bind to repetitive carbohydrate structures on the target cell surface." FC2 was mainly enriched in "Regulation of barbed end actin filament capping" and "diseases associated with surfactant metabolism." FC3 was primarily enriched in "Regulation of axon diameter" and "relaxin receptors" (Fig. 2F and G).

Integration of bulk-seq data to refine differential gene identification

In an effort to narrow down the list of differential genes implicated in IDD, we integrated additional nucleus pulposus bulk-seq data with our previously identified differential genes from the three functional fibro NPC subgroups. This comprehensive approach involved taking the intersection of differential genes identified in the bulk-seq analysis with the cumulative differential genes from the FC subgroups, resulting in the identification of four target genes: *TCF19*, *GDF15*, *RNMT*, and *C12orf45*. Visualization of these genes through volcano plots and heatmaps clearly demonstrated their upregulated expression in the IDD disease group compared to controls (Fig. 3A and B), signifying their potential role in the pathogenesis of IDD. Further analysis aimed to map these differential genes back to their respective FC subgroups within the single-cell data. This investigation revealed a significant upregulation of *TCF19* within the FC2 subgroup, whereas the remaining three genes—*GDF15*, *RNMT*, and *C12orf45*—were predominantly associated with the FC3 subgroup (Fig. 3C and D). Subsequently, we used RT-qPCR to validate the four aforementioned genes. Among them, the expression levels of *C12orf45*, *RNMT*, *GDF15*, and *TCF19* were elevated in the IDD group (Fig. 3E-H). The proportion of FC2 cells in the IDD group was high, and the number of these cells was greater than that of FC3 cells, so we chose to validate *TCF19*, which is specifically expressed in FC2 cells, at the protein level. Ultimately, we found that the protein expression level of TCF19 was elevated in the IDD group (Fig. 3I and J).

Pseudotime analysis of fibro NPCs in IDD

In order to delineate the progression dynamics within fibro NPCs populations in IDD, we conducted a pseudotime analysis. The analysis stratified fibro NPCs into seven distinct subpopulations (Fig. 4A), and trajectory analysis confirmed a transition within fibro NPCs from a normal to a diseased state (Fig. 4B). This transition was evident as cells progressed along the pseudotime axis, indicating a dynamic shift in gene expression corresponding to IDD pathogenesis. Further examination of the trajectory origins revealed that cells at the initial stages of the trajectory were typical of a normal state, whereas cells positioned at later stages were increasingly representative of the diseased state. At the same time, we also found that FC2 cells are mainly distributed on the key branch transitioning from normal to disease states (Fig. 4C), further indicating that FC2 cells may play an important role in the progression of IDD. Intriguingly, BEAM analysis, which investigates branching points in the trajectory for significant gene expression changes, highlighted that *TCF19* was uniquely positioned in a transitional state (Fig. 4D). This implies that *TCF19* may play a pivotal role in the transition of fibro NPCs from a normal to a degenerative state in IDD. Furthermore, we examined the expression levels of *TCF19*, *GDF15*, *RNMT*, and *C12orf45* on the simulated trajectory and found that only *TCF19* had an increased expression level at the end of the simulated trajectory, primarily expressed in FC2 cells (Figs. 4E-H).

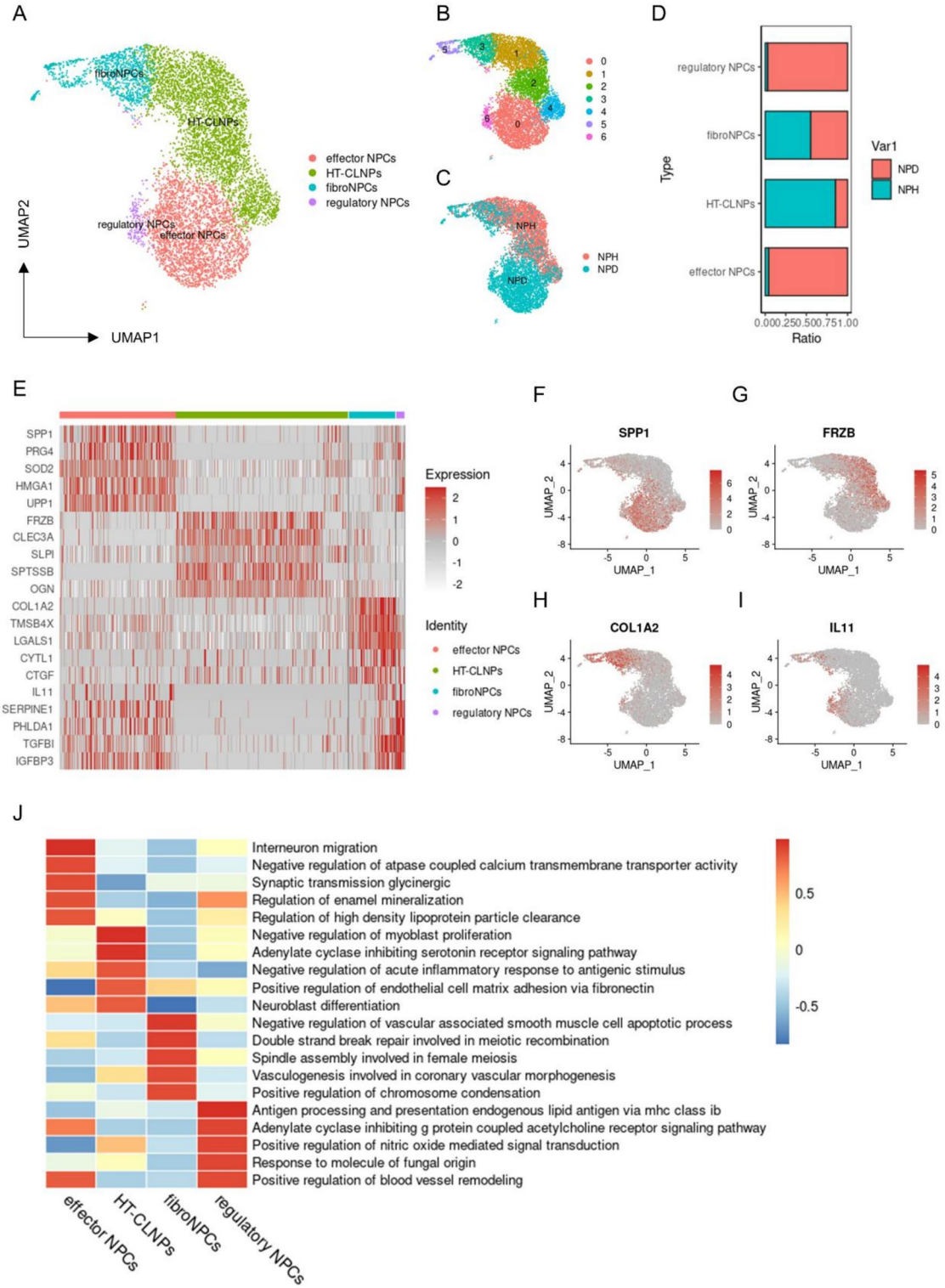

Fig. 1. Single-Cell Atlas of Nucleus Pulposus Cells in IDD. (**A**) UMAP visualization showing the distribution of NPCs clustered into distinct groups. (**B**) UMAP plots showing the distribution of NPCs clustered into Seurat clusters. (**C**) UMAP plots comparing the cellular heterogeneity in IDD versus normal disc tissue. (**D**) Proportion of cell types in healthy and IDD conditions. (**E**) Identification of cell types, with each type annotated according to specific marker genes. (**F**) SPP1 serves as a marker gene for effector NPCs. (**G**) FRZB serves as a marker gene for HT-CLNPs. (**H**) COL1A2 serves as a marker gene for fibro NPCs. (**I**) IL11 serves as a marker gene for regulatory NPCs. (**J**) Based on the GOBP GSVA analysis, red indicates pathway activation, and blue indicates pathway inactivation.

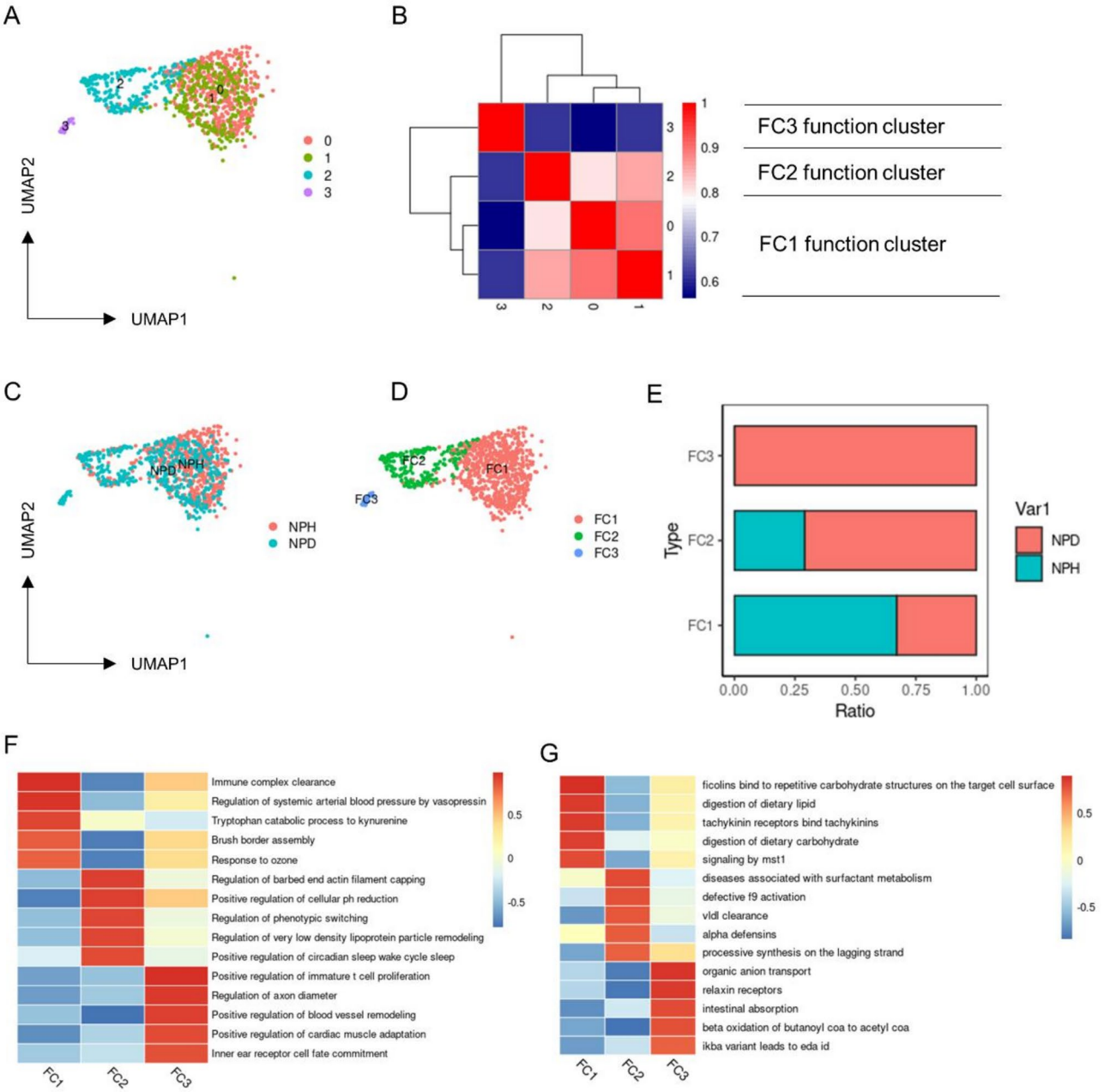

Fig. 2. fibro NPCs Subgroup Analysis. (**A**) Dimensional reduction clustering identifies four fibro NPCs subclusters indicative of unique transcriptional profiles within IDD and healthy controls. (**B**) Heatmap representation of subgroup gene expression similarity, delineating three functional subgroups within fibro NPCs based on differential gene expression patterns. (**C**) Differential UMAP plots of IDD versus control groups. (**D**) Differential functional subtype UMAP plots (**E**) Proportion of functional subtype in healthy and IDD conditions. (**F**) Based on the GOBP GSVA analysis, red indicates pathway activation, and blue indicates pathway inactivation. (**G**) Based on the KEGG GSVA analysis, red indicates pathway activation, and blue indicates pathway inactivation.

Cellular communication analysis in IDD

Our investigation into the cellular communication networks within NPCs revealed a marked difference in interaction intensity between IDD and healthy disc tissue. To further elucidate the role of *TCF19*, we divided fibro NPCs into *TCF19*-negative fibro NPCs and *TCF19*-positive fibro NPCs based on *TCF19* expression levels, and established a cell communication network. Analysis using CellChat highlighted a complex web of cell-to-cell communication that was significantly more pronounced in the IDD disease group (Fig. 5A and B), indicating an active cellular microenvironment in degenerated discs. To explore the intensity of communication between various cells, we created a heat map and found that the strongest communication was between regulator NPCs and other cells (Fig. 5C). When examining the differential pathways of cellular interaction between the disease and

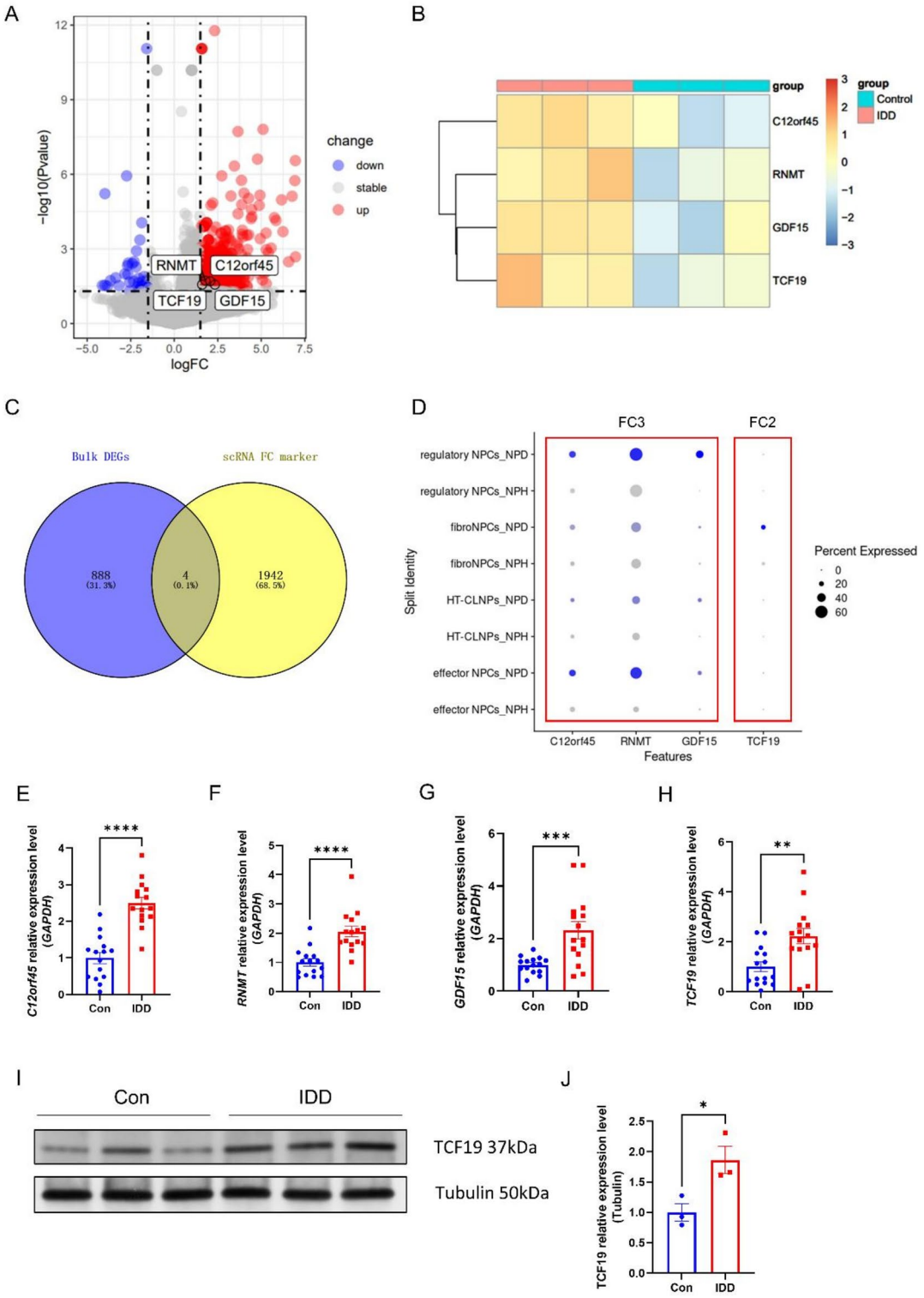

Fig. 3. Integration of Single-Cell and Bulk-seq Data Identifies Key IDD Targets. (**A**) Volcano plot showcasing differential gene expression between IDD and control samples, with significant upregulation of TCF19, GDF15, RNMT, and C12orf45 in IDD samples. (**B**) Heatmap illustrating the expression levels of TCF19, GDF15, RNMT, and C12orf45. (**C**) Intersection analysis of differentially expressed genes from single-cell and bulk-seq data. (**D**) Dot plot indicating the expression levels of targeted marker genes for NPC functional subtypes. (**E**–**H**) RT-qPCR validation of increased mRNA expression of C12orf45, RNMT, GDF15, and TCF19 in IDD nucleus pulposus tissues. (**I**–**J**) Western Blot analysis confirming the upregulation of TCF19 protein in IDD compared to control tissues. **** means $P < 0.0001$. *** means $P < 0.001$. ** means $P < 0.01$. * mean $P < 0.05$.

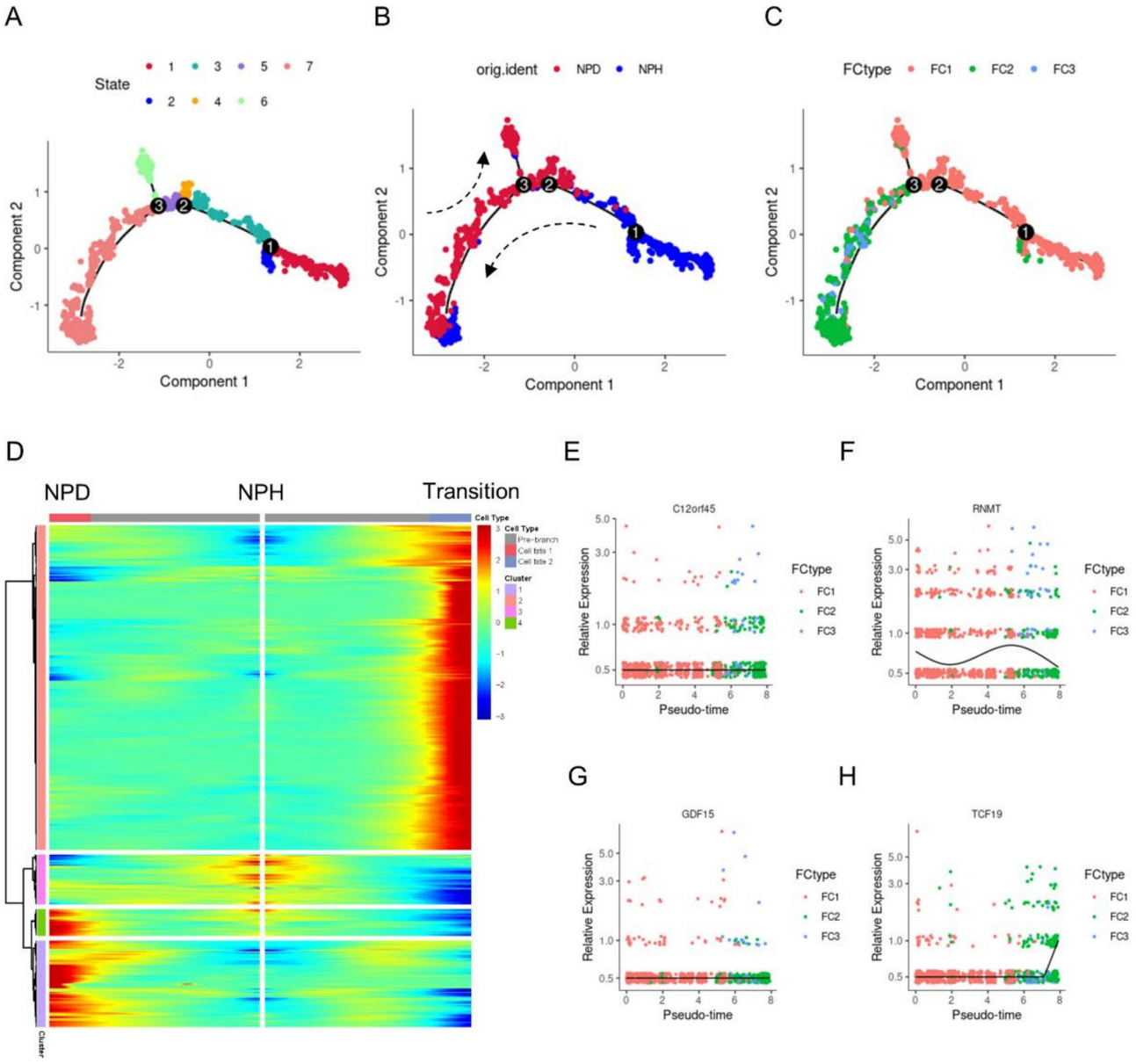

Fig. 4. Elucidation of NPC Subtype Dynamics via Pseudotime Analysis. (**A**) Trajectory map classifying seven NPC states within pseudotime. (**B**) Trajectory map classifying two NPC groups within pseudotime. (**C**) Trajectory map classifying three NPC function clusters within pseudotime. (**D**) BEAM analysis heatmap. Red indicates high gene expression levels, while blue indicates low gene expression levels. (**E**) The expression level of C12orf45 along the pseudotime axis. (**F**) The expression level of RNMT along the pseudotime axis. (**G**) The expression level of GDF15 along the pseudotime axis. (**H**) The expression level of TCF19 along the pseudotime axis.

normal states, significant pathways were depicted in a relative information flow (Fig. 5D). These pathways were characterized by their specific contribution to the altered cell signaling in the IDD context. Moreover, a detailed pathway analysis focusing on interactions within various NPC subgroups brought to light a pathway that was particularly enriched in fibro NPCs associated with the pathological state. This pathway was dominated by the secretion of the protein FN1, which was notably concentrated within the fibro NPCs population. Subsequently, we measured the concentration of FN1 in the plasma of individuals diagnosed with IDD and found that the concentration of FN1 in IDD plasma was higher than that in normal plasma (Fig. 5E). We primarily focused on the communication states of various cells within the FN1 pathway in the IDD group and discovered that effector NPCs and regulatory NPCs were in an active signal-sending state (Fig. 5F). Additionally, we identified the presence of an FN1-SDC4 receptor-ligand pair in *TCF19*-positive fibro NPCs (Fig. 5G). This suggests that TCF19 might upregulate SDC4 and mediate the activation of the FN1 pathway, thereby promoting intervertebral disc degeneration.

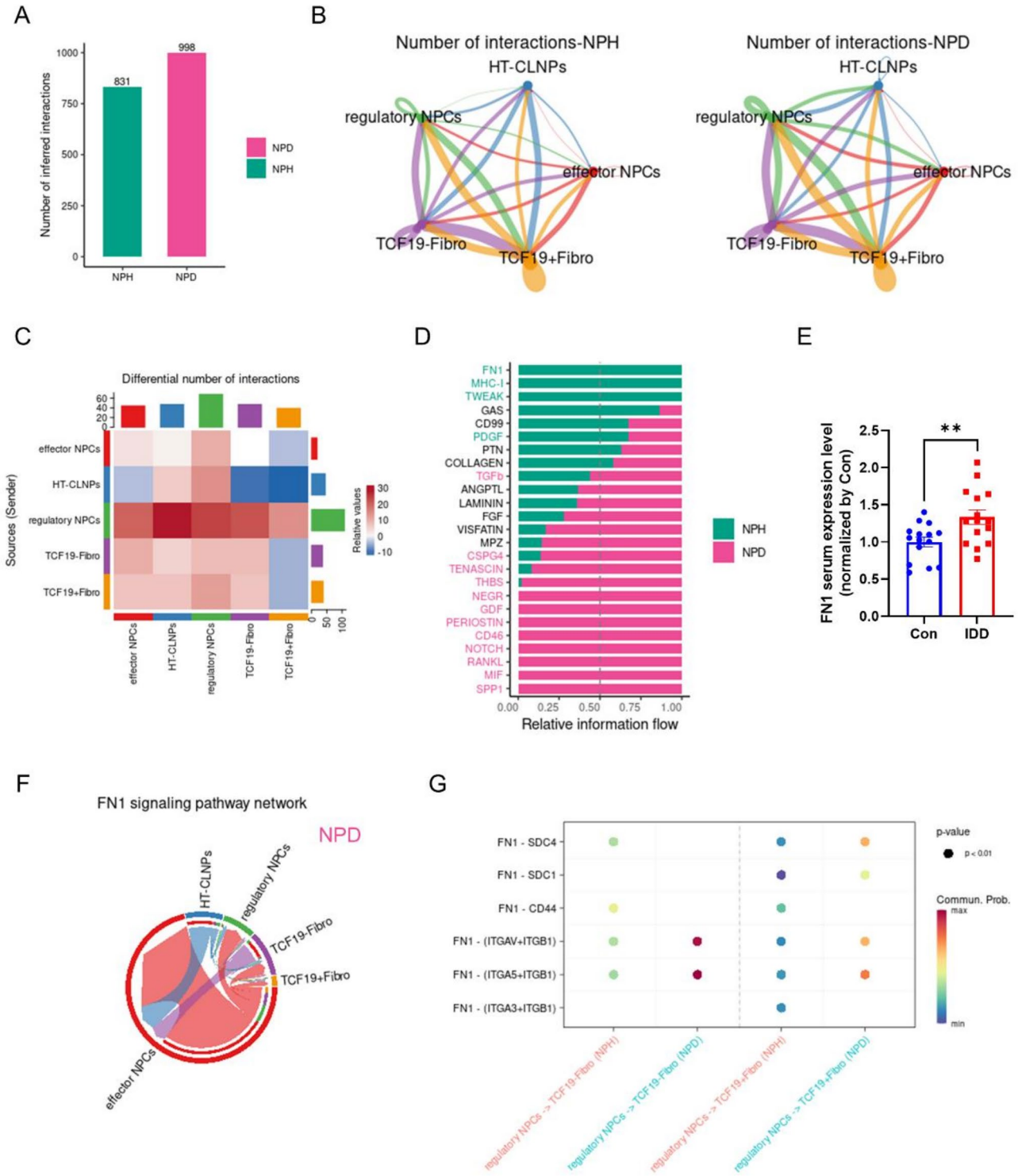

Fig. 5. Elucidation of Enhanced Cellular Communication. (**A**) The number of cell communications in the IDD group and normal group. (**B**) The communication network among various cells. (**C**) Heatmap of communication strength between different cells. (**D**) Communication strength of various pathways between cells. (**E**) Serum concentration of FN1 in the IDD group and normal group. (**F**) Communication network of FN1 among different cells in the IDD group. (**G**) Dot plot of FN1-related receptor-ligand pairs, where red indicates high communication strength and blue indicates low communication strength. ** means $P < 0.01$.

Knockdown of Tcf19 alleviates IDD

To investigate the relationship between Tcf19 and intervertebral disc degeneration (IDD), we established an IDD rat model. An overview of the animal experimental design is shown in Fig. 6A. We utilized adeno-associated virus (AAV) carrying shRNA to achieve knockdown of Tcf19. The results demonstrated a significant reduction in Tcf19 mRNA levels in the knockdown group compared to the control group (Fig. 6B). Following successful induction of IDD, the nucleus pulposus (NP) exhibited substantial degeneration. However, knockdown of Tcf19 significantly alleviated these degenerative changes (Fig. 6C and D), indicating that Tcf19 plays a crucial role in the progression of IDD. As a transcription factor, Tcf19 may initiate the transcription of downstream genes, leading to apoptosis in NP cells and contributing to notable disc degeneration. Furthermore, the expression level of Collagen X was markedly decreased in the Tcf19 knockdown group (Fig. 6E and G), suggesting an improvement in abnormal collagen deposition due to Tcf19 knockdown. Additionally, the expression level of MMP13 was also significantly reduced in the knockdown group (Fig. 6F and H), indicating an amelioration of the inflammatory response associated with Tcf19 knockdown. In summary, these results collectively demonstrate that knockdown of Tcf19 effectively mitigates nucleus pulposus degeneration, providing insights into potential therapeutic strategies for IDD by targeting this transcription factor.

Discussion

The findings from our comprehensive study have provided a detailed landscape of the cellular and molecular alterations occurring in IDD. By integrating single-cell RNA sequencing with bulk-seq data, we have uncovered not only the heterogeneity within nucleus pulposus cells (NPCs) but also identified critical genes and pathways that may drive the pathogenesis of IDD[17–21].

Our single-cell analysis delineated four distinct subtypes of NPCs, which included effector NPCs, HT-CLNPs, fibroNPCs, and regulatory NPCs. The discovery of these subtypes is significant, as it highlights the complexity of the NPC population within the degenerating disc and their potential specialized roles in disease progression. The identification of subtype-specific marker genes provides a valuable resource for future studies targeting these cells for therapeutic interventions.

Integration of bulk-seq data allowed us to narrow down a list of differentially expressed genes, leading to the identification of four target genes—*TCF19*, *GDF15*, *RNMT*, and *C12orf45*. These genes showed a marked upregulation in IDD and were validated through qPCR, suggesting their involvement in the degenerative processes of the disc[22–31]. Notably, *TCF19* emerged as a gene of particular interest due to its significant upregulation in a transitional state of NPCs, highlighting its potential role in the progression of IDD[22,24,25,31].

The cell communication network analysis revealed enhanced signaling interactions within the IDD group, with FN1 identified as a key mediator of this communication. The elevated levels of FN1 in the plasma of IDD patients underscore its potential as a biomarker and its role in the pathophysiology of IDD.

With the development of single-cell sequencing technology, more and more research is focusing on the gene transcription characteristics of IDD at the single-cell level. Studies from Europe and America have confirmed the importance of NPC in the progression of IDD, which is consistent with the conclusions of our research. There is also a significant amount of research proving that changes in gene transcription characteristics occur in NPC, which significantly promote the progression of IDD; this aligns with our findings as well. Our study identifies TCF19 as a new therapeutic target for treating IDD and indicates a direction for future drug development.

However, while our study has shed light on the intricate cellular and molecular mechanisms of IDD, it also opens up new avenues for research. The functional implications of the identified NPC subtypes and their interactions within the disc environment, along with the role of the target genes in disease progression, warrant further investigation[6,7,32–34]. Moreover, the therapeutic potential of modulating the identified signaling pathways and gene expression changes presents a promising area for future exploration[2,6,10,11,34–37].

In conclusion, our multidimensional approach has provided new insights into the biological underpinnings of IDD. The translational implications of our findings could pave the way for improved diagnostics and the development of more precise, targeted treatments for patients suffering from disc degeneration, thereby improving their quality of life.

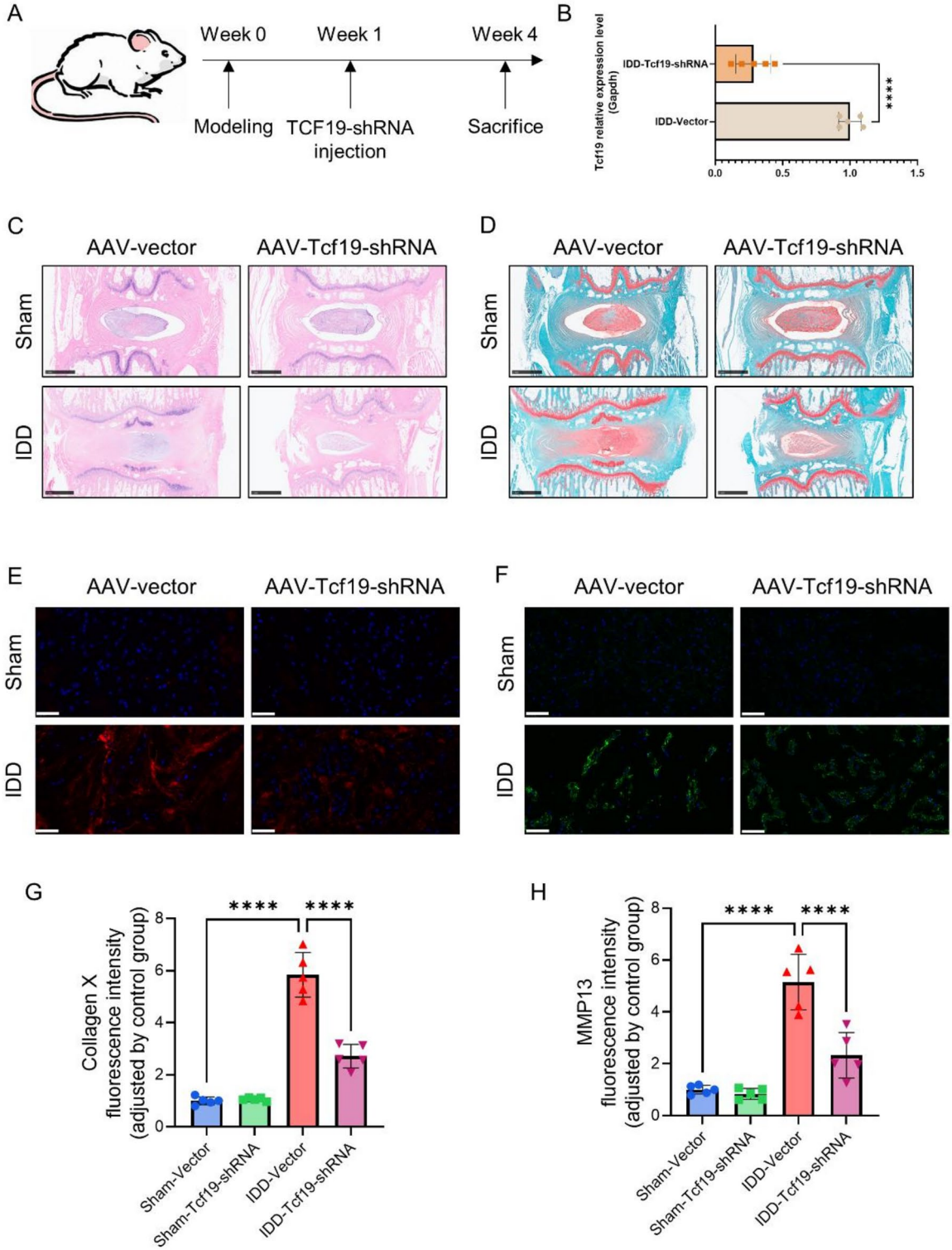

Fig. 6. Knockdown of Tcf19 alleviates IDD progression. (**A**) Schematic diagram of the animal experiment model. (**B**) Expression levels of Tcf19 in the IDD-vector group and IDD-Tcf19-shRNA group. (**C**) HE staining of the nucleus pulposus in Sham-vector group, Sham-Tcf19-shRNA group, IDD-vector group, and IDD-Tcf19-shRNA group. Scale bar is 1 mm. (**D**) Safranin O/Fast Green staining of the nucleus pulposus in Sham-vector group, Sham-Tcf19-shRNA group, IDD-vector group, and IDD-Tcf19-shRNA group. Scale bar is 1 mm. (**E**) Collagen X immunofluorescence of the nucleus pulposus in Sham-vector group, Sham-Tcf19-shRNA group, IDD-vector group, and IDD-Tcf19-shRNA group. Red represents Collagen X, blue represents DAPI. Scale bar is 50 μm. (**F**) MMP13 immunofluorescence of the nucleus pulposus in Sham-vector group, Sham-Tcf19-shRNA group, IDD-vector group, and IDD-Tcf19-shRNA group. Green represents MMP13, blue represents DAPI. Scale bar is 50 μm. (**G**) Immunofluorescence statistical results of Collagen X. (**H**) Immunofluorescence statistical results of MMP13. **** means $P < 0.0001$.

Data availability

Sequence data that support the findings of this study have been deposited in the GEO database with the primary accession code GSE199866 and GSE186542.

Received: 26 February 2025; Accepted: 5 May 2025
Published online: 08 May 2025

References

1. Xin, J. et al. Treatment of intervertebral disc degeneration. *Orthop. Surg.* **14**, 1271–1280. https://doi.org/10.1111/os.13254 (2022).
2. Ohnishi, T., Iwasaki, N. & Sudo, H. Causes of and molecular targets for the treatment of intervertebral disc degeneration: A review. *Cells* **11**, (2022). https://doi.org/10.3390/cells11030394
3. Liu, T. H., Liu, Y. Q. & Peng, B. G. Cervical intervertebral disc degeneration and dizziness. *World J. Clin. Cases* **9**, 2146–2152. https://doi.org/10.12998/wjcc.v9.i9.2146 (2021).
4. Gushcha, A. O. & Yusupova, A. R. [Modern concepts of intervertebral disc degeneration]. *Zh Vopr Neirokhir Im N N Burdenko.* **84**, 112–117. https://doi.org/10.17116/neiro202084061112 (2020).
5. Zheng, J. et al. Reactive oxygen species mediate low back pain by upregulating substance P in intervertebral disc degeneration. *Oxid. Med. Cell. Longev.* **2021** (6681815). https://doi.org/10.1155/2021/6681815 (2021).
6. Zhang, C. et al. Inflammatory cytokine and catabolic enzyme expression in a goat model of intervertebral disc degeneration. *J. Orthop. Res.* **38**, 2521–2531. https://doi.org/10.1002/jor.24639 (2020).
7. Yang, S. et al. Regulating pyroptosis by mesenchymal stem cells and extracellular vesicles: A promising strategy to alleviate intervertebral disc degeneration. *Biomed. Pharmacother.* **170**, 116001. https://doi.org/10.1016/j.biopha.2023.116001 (2024).
8. Wang, D. et al. Single-cell transcriptomics reveals heterogeneity and intercellular crosstalk in human intervertebral disc degeneration. *iScience* **26**, 106692. https://doi.org/10.1016/j.isci.2023.106692 (2023).
9. Ohnishi, T. et al. A review: methodologies to promote the differentiation of mesenchymal stem cells for the regeneration of intervertebral disc cells following intervertebral disc degeneration. *Cells* **12** https://doi.org/10.3390/cells12172161 (2023).
10. Lu, L. et al. Mesenchymal stem cell-derived exosomes as a novel strategy for the treatment of intervertebral disc degeneration. *Front. Cell. Dev. Biol.* **9**, 770510. https://doi.org/10.3389/fcell.2021.770510 (2021).
11. Liang, H., Yang, X., Liu, C., Sun, Z. & Wang, X. Effect of NF-kB signaling pathway on the expression of MIF, TNF-alpha, IL-6 in the regulation of intervertebral disc degeneration. *J. Musculoskelet. Neuronal Interact.* **18**, 551–556 (2018).
12. Li, Z. Y. et al. Chronic spinal cord compression associated with intervertebral disc degeneration in SPARC-null mice. *Neural Regen Res.* **18**, 634–642. https://doi.org/10.4103/1673-5374.350210 (2023).
13. Xiang, H., Yan, F. & Liu, H. The genetic association identified between intervertebral disc degeneration and associated risk factors based on a systems biology approach. *Spine (Phila Pa. 1976).* **47**, E370–E384. https://doi.org/10.1097/BRS.0000000000004312 (2022).
14. Mo, S. et al. KEGG-expressed genes and pathways in intervertebral disc degeneration: Protocol for a systematic review and data mining. *Med. (Baltim).* **98**, e15796. https://doi.org/10.1097/MD.0000000000015796 (2019).
15. Hu, X. et al. Single-cell sequencing: New insights for intervertebral disc degeneration. *Biomed. Pharmacother.* **165**, 115224. https://doi.org/10.1016/j.biopha.2023.115224 (2023).
16. Henry, G. H. et al. A cellular anatomy of the normal adult human prostate and prostatic urethra. *Cell. Rep.* **25**(12), 3530–3542e5. https://doi.org/10.1016/j.celrep.2018.11.086 (2018).
17. Calió, M., Gantenbein, B., Egli, M., Poveda, L. & Ille, F. The cellular composition of bovine coccygeal intervertebral discs: A comprehensive Single-Cell RNAseq analysis. *Int. J. Mol. Sci.* **22**(9). https://doi.org/10.3390/ijms22094917 (2021).
18. Joseph, D. B. et al. Urethral luminal epithelia are castration-insensitive cells of the proximal prostate. *Prostate* **80**(11), 872–884. https://doi.org/10.1002/pros.24020 (2020).
19. Branney, J., Breen, A., du Rose, A., Mowlem, P. & Breen, A. Disc degeneration and cervical spine intervertebral motion: A cross-sectional study in patients with neck pain and matched healthy controls. *J. Funct. Morphol. Kinesiol.* **9** https://doi.org/10.3390/jfmk9010055 (2024).
20. Alini, M., Diwan, A. D., Erwin, W. M., Little, C. B. & Melrose, J. An update on animal models of intervertebral disc degeneration and low back pain: Exploring the potential of artificial intelligence to improve research analysis and development of prospective therapeutics. *JOR Spine* **6**, e1230. https://doi.org/10.1002/jsp2.1230 (2023).
21. Fernandes, L. M. et al. Single-cell RNA-seq identifies unique transcriptional landscapes of human nucleus pulposus and annulus fibrosus cells. *Sci. Rep.* **10**(1), 15263. https://doi.org/10.1038/s41598-020-72261-7 (2020).
22. Yang, G. H. et al. TCF19 impacts a network of inflammatory and DNA damage response genes in the pancreatic beta-Cell. *Metabolites* **11** https://doi.org/10.3390/metabo11080513 (2021).
23. Steinmetz, J., Stemmler, A., Hennig, C. L., Symmank, J. & Jacobs, C. GDF15 contributes to the regulation of the mechanosensitive responses of PdL fibroblasts through the modulation of IL-37. *Dent. J. (Basel)* **12** https://doi.org/10.3390/dj12020039 (2024).
24. Ruan, X. et al. Multidimensional data analysis revealed thyroiditis-associated TCF19 SNP rs2073724 as a highly ranked protective variant in thyroid cancer. *Aging (Albany NY)* **16** https://doi.org/10.18632/aging.205718 (2024).
25. Ma, X. et al. Targeting TCF19 sensitizes MSI endometrial cancer to anti-PD-1 therapy by alleviating CD8(+) T cell exhaustion via TRIM14-IFN-beta axis. *Cell. Rep.* **42**, 112944. https://doi.org/10.1016/j.celrep.2023.112944 (2023).
26. Liang, S., Almohammed, R. & Cowling, V. H. The RNA cap methyltransferases RNMT and CMTR1 co-ordinate gene expression during neural differentiation. *Biochem. Soc. Trans.* **51**, 1131–1141. https://doi.org/10.1042/BST20221154 (2023).
27. Kosum, P. et al. GDF-15: a novel biomarker of heart failure predicts short-term and long-term heart-failure rehospitalization and short-term mortality in patients with acute heart failure syndrome. *BMC Cardiovasc. Disord.* **24**, 151. https://doi.org/10.1186/s12872-024-03802-5 (2024).
28. Kim, H. R. et al. Association between serum GDF-15 and cognitive dysfunction in Hemodialysis patients. *Biomedicines* **12** https://doi.org/10.3390/biomedicines12020358 (2024).
29. Galloway, A. et al. Upregulation of RNA cap methyltransferase RNMT drives ribosome biogenesis during T cell activation. *Nucleic Acids Res.* **49**, 6722–6738. https://doi.org/10.1093/nar/gkab465 (2021).
30. de Avila, D. X. et al. Growth differentiation factor-15 (GDF-15) and clinical outcomes in patients with chronic heart failure. *J. Card Fail.* https://doi.org/10.1016/j.cardfail.2024.02.026 (2024).
31. Cheng, X. et al. Immunotherapeutic value of transcription factor 19 (TCF19) associated with renal clear cell carcinoma: A comprehensive analysis of 33 human Cancer cases. *J. Oncol.* **2022**(1488165). https://doi.org/10.1155/2022/1488165 (2022).
32. Yin, S. et al. Inhibition of both endplate nutritional pathways results in intervertebral disc degeneration in a goat model. *J. Orthop. Surg. Res.* **14** https://doi.org/10.1186/s13018-019-1188-8 (2019).
33. Wu, Y. et al. Senolytics: eliminating senescent cells and alleviating intervertebral disc degeneration. *Front. Bioeng. Biotechnol.* **10**, 823945. https://doi.org/10.3389/fbioe.2022.823945 (2022).
34. Su, Q. et al. A novel rat model of vertebral inflammation-induced intervertebral disc degeneration mediated by activating cGAS/STING molecular pathway. *J. Cell. Mol. Med.* **25**, 9567–9585. https://doi.org/10.1111/jcmm.16898 (2021).

35. Silva, M. J. & Holguin, N. Aging aggravates intervertebral disc degeneration by regulating transcription factors toward chondrogenesis. *FASEB J.* **34**, 1970–1982. https://doi.org/10.1096/fj.201902109R (2020).
36. Ogon, I. et al. Association between lumbar segmental mobility and intervertebral disc degeneration quantified by magnetic resonance imaging T2 mapping. *N Am. Spine Soc. J.* **5**, 100044. https://doi.org/10.1016/j.xnsj.2020.100044 (2021).
37. NaPier, Z. et al. Omega-3 fatty acid supplementation reduces intervertebral disc degeneration. *Med. Sci. Monit.* **25**, 9531–9537. https://doi.org/10.12659/MSM.918649 (2019).

Author contributions
Xianwei He and Liwei Wu wrote the main manuscript text. Xianwei He prepared Figs. 1, 2 and 3. Liwei Wu and Hao Zhou prepared Figs. 3, 4, 5 and 6. All authors reviewed the manuscript.

Declarations

Competing interests
The authors declare no competing interests.

Ethical approval
The Permission of the Hospital Ethics Committee was obtained by the Jinshan hospital's ethics committee.

Human and animal rights
The study is reported in accordance with ARRIVE guidelines, and approved by Jinshan hospital's animal center ethics committee (2023-05ARBB). The study is performed in accordance with Declaration of Helsinki.

Additional information
Supplementary Information The online version contains supplementary material available at https://doi.org/10.1038/s41598-025-01180-2.

Correspondence and requests for materials should be addressed to L.W. or H.Z.